An evaluation model for aboveground biomass based on Hyperspectral Data from field and TM8 in Khorchin grassland, China

Xiaohua Zhang[1,2‡], Meirong Tian [2‡*], Xiuli Chen[3‡], Yongjun Fan[3], Jianjun Ma[4], Danlu Xing[2]

1 College of Applied Meteorology, Nanjing university of Information Science & Technology, Nanjing, China;

2 Nanjing Institute of Environmental Science, Ministry of Ecology and Environment of China, Nanjing, China;

3 Baotou Teacher's college, Biological Science and Technology Institute, Baotou , Inner Mongolia, China;

4 College of Life Science, Lang Fang Normal University, Lang fang, China;

‡ *These authors are co-first authors on this work.*

* tmr@nies.org

Abstract

Biomass is an important indicator for monitoring vegetation degradation and productivity. This study tests the applicability of Hyperspectral Remote-Sensing in situ measurements for high-precision estimation aboveground biomass (AGB) on regional scales of Khorchin grassland landscape in Inner Mongolia, China. Field experiments were carried out which collected hyperspectral data with a portable visible/NIR hyperspectral spectrometer (SOC 710), and collected aboveground net primary productivity (ANPP). Ground spectral models were then developed to estimate ANPP from the normalized difference vegetation index (NDVI), which was measured in the field following the same method as that of the Thematic Mapper(TM) from the Landsat 8 land imager (TM_NDVI). Regression analysis was used to assess the relationship between ANPP and NDVI based on coefficients of determination (R^2) and error analysis. The estimation of ANPP had unique optimal regression models. By comparing the different spectral inversion models, we selected an exponential model associating ANPP with NDVI (ANPP = 12.523*e3.370*(0.462*TM_NDVI+0.413), standard error = 24.74 g m-2, R^2 = 0.636, P < 0.001). This study suggests that the model can be used to monitor the condition and estimate the productivity of grassland at regional scales. The results still show a high potential to map grassland degradation proxies on the ground hyperspectral model. Thus, this study presents biomass hyperspectral inversion technology to remotely detect and monitor grassland degradation and productivity at high precision.

Key words: Biomass, Field hyperspectral, Remote sensing, Khorchin

Introduction

The tools for remotely sensing of vegetation have evolved significantly in recent decades[1], and spectral imaging has become increasingly popular in remote-sensing research for correlating spectral data with the biophysical properties of vegetation. Hyperspectral remote-sensing data have subsequently been widely used to estimate vegetation biomass[2-5], vegetation cover (VC)[6-7], nitrogen content[8], and the leaf area index of vegetation[1,9].

The accurate estimation of aboveground net primary productivity (ANPP) is an active area of research and can provide valuable information about the productivity and ecosystem service value of grassland [10]. ANPP is an important impact factor for desertification and are often used as indicators for monitoring and evaluating grassland productivity and degradation [11]. The present study aimed to develop models for estimating biomass and VC based on satellite data, which allow an assessment over large areas at a low cost [12]. Desertification in the Khorchin grassland is becoming worse with the rapid expansion of the population, overgrazing and the warmer and drier trend associated with climate change [13]. The accurate estimation of the biomass of the grassland over large areas using remotely sensed data is thus very important for monitoring desertification and for improving the scientific management of grassland ecological resources.

Remote-sensing data have been transformed and combined into various spectral vegetation indices that are used as predictors of parameters, such as the normalised difference vegetation index (NDVI), ratio vegetation index, perpendicular vegetation index, soil adjusted vegetation index, and transformed soil adjusted vegetation index [14-17]. Most studies apply NDVI because it minimises the effects of topography[18] and is more reliable for the estimation of biomass of ecosystems/habitats dominated by grasses when the grasses are actively growing [9,19]. The NDVI is thus widely used to characterise grass ecosystems and to estimate biomass and VC[3,4,19-23].

NDVI have been determined from data sets collected by various satellite instruments, such as the Landsat Thematic Mapper (TM), the National Oceanic and Atmospheric Administration/Advanced Very High Resolution Radiometer (NOAA/AVHRR), MODIS, Gaofen-2 and the Moderate Resolution Imaging Spectro radiometer[9,24]. The Landsat 8 with narrowband indices are highly suitable to be chosen to map AGB accurately, because the narrowband indices have led to significant improvements in the predictive capability of models, and hyperspectral data from aerial imagery or field spectrometry have the potential to estimate the biophysical properties of rangeland or steppe vegetation with a greater accuracy than broadband indices [3,4,23,25-26].

In order to improve the accuracy of biomass estimation, the measurements of ground reflectance have been used to estimate biomass in grasslands and steppes since the 1970s [27], but ground spectral reflectance can be influenced by variable factors of the landscape such as the distribution of plant communities [28], soil colour [29], hydrology[30], and topography[31], and sensor radiance may be strongly affected by atmospheric scattering[32]. For these reasons, various regression models have been established for associating vegetation indices with biomass in different areas. Relationships have been established between remote-sensing data and the biophysical properties of vegetation, mostly linear or non-linear, that have greatly improved the accuracy of biomass estimates and that have determined patterns of grassland productivity in various regions [6,33-37].

Taking into account the advantages and disadvantages of the current remote sensing sources to estimate AGB, In this study, we present a remote sensing approach for estimating and monitoring AGB in meadows and pastures during the growing season. We used remote sensing of Landsat 8 and ground hyperspectral to calculate the normalized difference vegetation index (NDVI), and on-field aboveground net primary production (ANPP) measurements to establish an empirica1 exponential model to estimate spatial ANPP across the entire Khorchin grassland.

The main objectives of this study are: (i) to analyse the relationship of the ground narrowband NDVI with ANPP and then to develop the most suitable ground spectral models for evaluating ANPP over a large area of the Khorchin steppe, and (ii) to use the ANPP model to understand the biocapacity of the Khorchin grassland for providing technical support for determining a reasonable grazing intensity and guiding the development of the livestock industry.

Materials and methods

Study area

The Khorchin grassland is located in the eastern section of the ecotone between crop production and animal husbandry, we choose the region of Bairin Youqi in Inner Mongolia of China as the study area (Fig. 1), which is an important component of the Khorchin grassland and is typically sensitive and fragile. Bairin Youqi has a semiarid, temperate, continental monsoon climate with mean annual temperature of 4.9 °C and mean annual precipitation of 358 mm (precipitation is less than evaporation). From low to high elevations, the distribution of vegetation is meadow, sandy vegetation, and low mountain grassland respectively. The dominant grassland species include *Achnatherum splendens* (*Trin.*) Nevskia, *Stipa capillata* Linn., *Leymus chinensis (Trin.)* Tzvel., and *Agropyron cristatum (Linn.)* Gaertn.

Fig. 1 Map of Inner Mongolia (left) and the location of the sampling sites in Bairin Youqi (right)

This study was carried out in the field of Khorchin grassland which was State-owned Land and did not involve endangered or protected species. Meanwhile, because this study supported by National Environmental Conservation Research Program, so the government of Bairin Youqi permitted and approved this study.

Collection of field data

Experimental setup

Field work was conducted during 15-30 July 2016, coinciding with the most productive period of vegetational growth. Based on the topography and land use, 39 plots were established that included large, homogeneous patches of vegetation and representative vegetational communities with different types of vegetation. The plot size was set at 30 × 30 m, equivalent to the size of a TM8 pixel. The plots contained a total of 173 quadrats of 1 × 1 m. The data collected were divided into 2 groups. Group one, which contained 153 quadrats were used to build the ground spectral model; group two, which contained 20 quadrats, were used for the accuracy test of the spectral inversion model. Meanwhile, within group one, the data of approximately two thirds of the total quadrats (n=115) were chosen randomly to build the model while the rest were used for testing the terrain model in terms of selecting the best fitting function and precision.

Field spectral data

The field data were collected using the SOC710 Hyperspectral Imaging System which Manufactured by Surface Optics Corporation in America. The SOC710 is a precision instrument with an integrated scanning system and analysis software that can quickly obtain high-quality hyperspectral images at visible to near-infrared (NIR) wavelengths in the range 0.4-1.0 μm. The system can be used under normal lighting conditions at variable exposures and gains. The SOC spectra were collected with a 10° field of view and at 1.2 m above the grass canopy. All spectral measurements were collected between 9:00 and 15:00 Beijing time under clear skies. Three measurements were taken for each sample of grass canopy. These spectra were standardised to spectra measured at approximately 10-minute intervals with a white board. The average of three replicates for each sample was used for the analysis.

Biomass measurements

After the spectral data had been recorded, the standing biomass was collected in the quadrats at each sample location. The fresh weight of green herbaceous material was recorded soon after clipping, the samples were then dried at 80 °C for 10-12 hours, and the dry masses of the samples were determined.

Image data acquisition, satellite data, and preprocessing

Biomass was assessed using TM8 data from the Landsat 8 land imager of the United States Geological Survey. The satellite data were acquired within the same time frame in which the field data had been collected, and the images were free of clouds and haze. Four suitable TM8 satellite scenes at PATH/ROWs 123/29, 123/30, 122/29, and 122/30 were analysed. The satellite data were geometrically rectified by a digital elevation model and ground-control points from Land Survey. The four TM8 scenes were processed for atmospheric correction with the Fast Line-of-sight Atmospheric Analysis of Spectral Hypercubes software package.

Data analysis

NDVI calculation

NDVI are commonly calculated from RED and NIR reflectance data [38]. We calculated the SOC_NDVI of the samples from SOC710 spectral reflectance using the ENVI 5.0 image analysis software. The method for calculating NDVI was the same as that used for calculating the TM_NDVI:

$$NDVI = \frac{NIR - RED}{NIR + RED} \qquad (1)$$

Where the RED and NIR bands correspond to wavelengths of 630-680 and 845-885 nm, respectively. Spectral reflectance data should be resampled within the scope of the RED and NIR bands.

Regression analyses

The regression analyses were carried out for the scatter diagrams of ANPP vs. SOC_NDVI, and SOC_NDVI vs. TM_NDVI. In study area, The 173 quadrats data were employed to obtain the regression model for ANPP vs. SOC_NDVI. Mean value of NDVI within a specific plot was calculated, and then the data of the total 39 plots (Fig. 1) were used in the regression analysis for SOC_NDVI vs. TM_NDVI.

The coefficient of determination (R^2) and the adjusted R^2 were used to test the strength and significance of the relationships between the field data and the corresponding data extracted from the satellite scenes. The standard error (SE, Eq. 2) of the prediction based on the independent test data and the coefficient of mean error (MEC, Eq. 3) were calculated to assess the accuracy of the developed models.

$$SE = \sqrt{\frac{\sum_{i=1}^{n}\left(y - y'\right)^2}{n}} \qquad (2)$$

$$MEC = \frac{\sum_{i=1}^{n}\left|\frac{y - y'}{y}\right|}{n} \qquad (3)$$

where y is a measured biomass, y′ is an estimated biomass for the test data, and n is the number of samples.

Results

Optimal ground spectral models and tests of model accuracy

The optimal ground spectral models for biomass

From the analysis and evaluation of the relationships between ANPP and SOC_NDVI computed from reflectance data obtained by the SOC710 in the field, we chose linear, logarithmic, power, and exponential functions to fit and optimise the regression equations for selecting the best regression model (Fig.2).

Fig.2 The Simulation Curves of the Regression Equation of the Training Samples

The relationships between ANPP and SOC_NDVI was significant ($P < 0.001$) for all functions and met the assumptions of the statistical analyses. The exponential model was superior for ANPP, with an R^2 of 0.636, indicated by bold type in Tables 1.

Table 1 Comparison of the regression equations between ANPP and SOC_NDVI.

	Linear	Logarithmic	Power	Exponential
n	115	115	115	115
Equation	$y = 443.297x - 166.610$	$y = 284.562\ln(x) + 248.525$	$y = 299.611x^{2.216}$	$\mathbf{y = 12.523e^{3.370x}}$
R^2	0.617	0.579	0.626	**0.636**
AdjustedR^2	0.614	0.575	0.623	0.633
$F(\alpha=0.01)$	182.255 ($P <$ 0.001)	155.181 ($P < 0.001$)	802.5746 ($P < 0.001$)	1089.7635($P <$ 0.001)

Note: n, number of samples; R^2,coefficients of determination; the best regression model is highlighted in bold.

Tests of model accuracy

The accuracy of the models was tested to obtain the best regression models. We used test sets of all field samples to analyse and evaluate the errors in the regression models (Table 2). A comparison of the predictive performances of the regression equations indicated by SE and MEC are presented in Table 2.

Table 2 Comparison of the errors of the regression equations.

	Linear	Logarithmic	Power	Exponential

ANPP	*n*	38	38	38	38
	SE (gm^{-2})	52.64	55.46	51.32	**49.22**
	MEC (%)	34.77	37.09	31.64	**30.01**

Note: *n*, number of samples; SE, standard error of prediction; MEC, coefficient of mean error; the SE and MEC of the best regression model for each vegetational parameter are highlighted in bold.

We determined the best models for ANPP based on R^2 and the independent validations. The exponential equation was optimal for ANPP (R^2 = 0.636, SE = 49.22gm^{-2}, MEC = 30.01%; Tables 1 and 2). Models with the following equations (Eqs. 4) were selected and used as the optimal ground spectral models for ANPP of the entire Khorchin grassland:

$$ANPP = 12.523 * e^{3.370 * SOC\_NDVI} \qquad (4)$$

The relationship between TM_NDVI and SOC_NDVI

The linear regression equation was selected based on the analysis of the TM_NDVI/SOC_NDVI scatter plot. The relationship between TM_NDVI and SOC_NDVI was significant, with an R^2 of 0.656 (P < 0.001) and met the assumptions of the statistical analyses (Table 4, Fig.3). The model with the following equation (Eq. 5) was selected for the relationship between TM_NDVI and SOC_NDVI for the entire Khorchin grassland:

$$SOC\_NDVI = 0.462*TM\_NDVI+0.413 \qquad (5)$$

Table 3 Regression equations between TM_NDVI and SOC_NDVI.

Equation	*n*	*R*	R^2	*F* (α=0.01)
y=0.462X+0.413	39	0.810	0.656	70.63，P < 0.001

Note: *n*, number of samples; *R*, R^2,coefficients of determination.

Fig. 3 Fitted curve of the best model for the relationship between SOC_NDVI and TM_NDVI.

Spectral inversion models

The spectral inversion models of TM8 for ANPP was calculated by Eqs. 4-5:

$$ANPP = 12.523 * e^{3.370*(0.462*TM\_NDVI+0.413)} \qquad (6)$$

To test the agreement between measured and predicted values, we applied Eqs. 6 to the TM8 NDVI greyscale image and obtained the patterns of ANPP distribution in the study area by grid computing. The test data sets were then converted into vector diagrams defined by geographic coordinates by geographic information system. The values at the test points were recorded in the distribution patterns as the corresponding pixels predicting values of ANPP. The relationship between actual and predicted values was used to evaluate the accuracy of model.

The correlation between the predicted and actual values was significant, as were the independent validations for predicting biomass (SE = 24.74, MEC = 18.61%; Fig.4). This study suggested that the spectral inversion models could be used to monitor grassland biomass at regional scales.

Fig. 4 Independent validation for predicting biomass (*n* = 20, *P* < 0.001). SE, standard error of

predicted biomass; MEC, coefficient of mean error.

Discussion

The main goal of this study was to establish more accurate models for estimating ANPP of the grassland in Khorchin. We chose the NDVI vegetation index, which can be calculated from spectral reflectance data acquired in the field and from data from Landsat TM7 Band 4 (TM4; 760-900 nm) and Band 3 (TM3; 630-690 nm) or from NOAA/AVHRR Channel 1 (580-680 nm) and Channel 2 (720-1100 nm)[39-41]. In a previous study, we also calculated the NDVI from data collected by a FieldSpec3 spectroradiometer (Analytical Spectral Devices, Boulder, USA), at spectral reflectances of 620-670 (RED) and 841-876 (NIR) nm [9]. To further improve the accuracy in the present study, we chose satellite data from Landsat 8(TM8), which have a higher geometric precision and signal-to-noise ratio than the other Landsat data, and used the SOC710 Hyperspectral Imaging System, which is more accurate than the FieldSpec3 spectroradiometer. The TM8 remotely sensed imaging data were only released in 2013, so they have not yet been widely applied to monitor vegetational biomass. This study applied the field data for monitoring the vegetation, thereby providing an informational baseline for this study area. The spectral inversion model was ideal, indicating that TM8 remote imaging can be used for research on vegetation biomass on a regional scale.

ANPP have their own optimal regression models based on the processing and statistical analysis of experimental data in the study area. The optimal equations for the estimation of ANPP (Fig.5) indicate that the relationship between SOC_NDVI and ANPP weakens at biomass >350 g m^{-2} for grassland. Estimates of biomass above these levels are inaccurate or unreliable and may be affected by the NDVI lower saturation phenomenon in areas of dense vegetation cover. When biomass exceed these levels, factors such as grass height and leaf area index must be considered, or a modified SOC_NDVI should be derived[42].

Fig. 5 Fitted curve of the best model for the relationship between ANPP and SOC_NDVI for the calibration sets

The ground spectral models for ANPP can be applied to TM8 images, because measured spectral characteristics of plants on the ground are intrinsically linked to those obtained by TM8 remote sensing. Grassland yield over large areas can be estimated based on the ground spectral model. The models, however, could be more accurate if field and satellite data are collected over several years rather than only for one year. Also, the field and satellite data should be acquired at the same time for maximal correspondence. In future field experiments, we will assess the collective influence of these vegetational characteristics and the NDVI on biomass prediction and will seek to obtain a modified NDVI for estimating the biomass of dense vegetation under natural conditions.

Conclusions

This study developed a relatively accurate model for estimating AGB and tests the applicability of hyperspectral data from field and TM8 to map AGB on regional scales by a regression analysis method. The methodology we adopted in the study was a first attempt to Retrieval of vegetation biomass from ground hyperspectral remote sensing in Khorchin grassland.

The accuracy of ground spectral inversion is affected by many factors, and the quality of the selected remote sensing image data has the greatest impact on the fitting accuracy of the model. Landsat 8 satellite data is selected for remote sensing data, which has higher geometric accuracy and signal-to-noise ratio than previous Landsat data, which effectively expands the application range of image data. In the aspect of imaging mode, the sweep pendulum design of OLI imager has good stability and improves the image quality, and in the aspect of geometric accuracy, L1T data product is a data product after precise correction, and the product accuracy has been greatly improved. In this paper, TM8 data is used to retrieve vegetation biomass, and the results show that calculated R^2 and SE and MEC values for various regression models vary among ground spectral models. By comparison, the exponential regression models we developed show a stronger relationship between spectral reflectance and ANPP. An exponential equation was optimal for estimating ANPP in the Khorchin grassland. Accuracy verification indicated that the relationship between the actual and predicted biomass was significant. Estimating ANPP with high accuracy based on NDVI derived from TM8 satellite data is thus possible, which accumulates experience for the application of TM8 data in vegetation monitoring field.

The accuracy of this technique depends on living, green biomass and not on senesced or dead biomass, so the timing of the acquisition of NDVI data is critical, and the model can possibly be improved if models are developed per vegetation types and using a larger range of ground data. In brief, this research shows the usefulness of hyperspectral data from field and TM8 to evaluate aboveground biomass at very high precision to provide theoretical and data support for RS monitoring, grassland governance and ecological restoration.

Acknowledgements

We would like to thank Xueping Pan, Kun Wang, and Maorong Tian for their help with the collection and identification of the grasses, and thank Jixi Gao and Yanmei Chen for their help with guiding techniques and methods.

References

1. Darvishzadeh, R, Skidmore, A, Atzberger, C, Wieren, S. V. Estimation of vegetation LAI from hyperspectral reflectance data: effects of soil type and plant architecture. International Journal of Applied Earth Observation and Geoinformation. 2008;10(3):358-373. https://doi.org/10.1016/j.jag.2008.02.005.
2. Mutanga O, Skidmore A K. Hyperspectral band depth analysis for a better estimation of grass biomass (Cenchrus ciliaris) measured under controlled laboratory conditions. International Journal of Applied Earth Observation and Geoinformation. 2004;5(2):87-96. https://doi.org/10.1016/j.jag.2004.01.001.
3. M.A.Cho, A.Skidmore, F.Corsi, S.E.Van wieren, I.Sobhan. Estimation of green grass/herb biomass from airborne hyperspectral imagery using spectral indices and partial least squares regression. International Journal of Applied Earth Observation and Geoinformation. 2007;9(4):414–424 https://doi.org/10.1016/j.jag.2007.02.001.
4. I.Numata, D.A.Roberts, O.A.Chadwick, J.P.Schimel, L.S.Galvao, J.V.Soares. Evaluation of hyperspectral data for pasture estimate in the Brazilian Amazon using field and imaging spectrometers. Remote Sensing of Environment. 2008; 112(4):1569-1583. https://doi.org/10.1016/j.rse.2007.08.014.
5. Gaia Vaglio Laurin, Johannes Balling, Piermaria Corona, Walter Mattioli, Dario Papale, Nicola Puletti, Maria Rizzo, John Truckenbrodt, Marcel Urban. Above-ground biomass prediction by Sentinel-1multitemporal data in central Italy with integration of ALOS2 and Sentinel-2 data. Appl. Remote Sens. 2018;12(1):016008. https://doi.org/10.1117/1.JRS.12.016008

6. M. Kenneth, M.Timothy, F.Lynn. Hyperspectral Mixture Modeling for Quantifying Sparse Vegetation Cover in Arid Environments. Remote Sensing of Environment. 2000; 72(3):360–374. https://doi.org/10.1016/S0034-4257(99)00112-1.
7. X.F. Zhang, C.H. Liao, J. Li, Q. Sun. Fractional vegetation cover estimation in arid and semi-arid environments using HJ-1 satellite hyperspectral data. International Journal of Applied Earth Observation and Geoinformation. 2013; 21:506–512. https://doi.org/10.1016/j.jag.2012.07.003 .
8. A. Ramoelo, A.K. Skidmore, M.A. Cho, R. Mathieu, I.M.A. Heitkönig, N. Dudeni-Tlhone, M. Schlerf, H.H.T. Prins. Non-linear partial least square regression increases the estimation accuracy of grass nitrogen and phosphorus using in situ hyperspectral and environmental data. ISPRS Journal of Photogrammetry and Remote Sensing. 2013;82:27–40. https://doi.org/10.1016/j.isprsjprs.2013.04.012.
9. S. Gao, Z. Niu, N. Huang X.H. Hou. Estimating the Leaf Area Index, height and biomass of maize using HJ-1 and RADARSAT-2. International Journal of Applied Earth Observation and Geoinformation. 2013; 24, 1–8.https://doi.org/10.1016/j.jag.2013.02.002.
10. J.X. Gao, Y.M. Chen, Sh. H. Lü, Ch. Y. Feng, X.L. Chang, Sh. X. Ye, J.D. Liu. A ground spectral model for estimating biomass at the peak of the growing season in Hulunbeier grassland, Inner Mongolia, China. International Journal of Remote Sensing. 2012 ;33(13): 4029–4043. https://doi.org/10.1080/01431161.2011.639401.
11. T.J. Cai, C.Y. Ju, Y.F. Yao. Quantitative estimation of vegetation coverage in Mu Us sandy land based on RS and GIS. Chinese Journal of Applied Ecology. 2005;16(12):2301-2305 (in Chinese with English abstract). http://en.cnki.com.cn/Article_en/CJFDTotal-STBC200302005.htm.
12. S. Eckert, M. Engesser. Assessing vegetation cover and biomass in restored erosion areas in Iceland using SPOT satellite data. Applied Geography. 2013;40: 179-190. https://doi.org/10.1016/j.apgeog.2013.02.015.
13. C.Y. Cao, D.M. Jiang, L.H. Zhu, Y.H. Nan. Degradation and diversity changes of meadow grassland in Keerqin Sandy Land. Acta Prat Aculturae Sinica. 2006;15(3):18-26 (in Chinese with English abstract). http://en.cnki.com.cn/Article_en/CJFDTotal-CYXB200603002.htm.
14. T.N. Carlson, D.A. Ripley. On the relation between NDVI, fractional vegetation cover, and leaf area index. Remote Sensing of Environment. 1997;62:241–252. https://doi.org/10.1016/S0034-4257(97)00104-1.
15. P.S. Thenkabail, R.B. Smith, E. De Pauw. Hyperspectral vegetation indices and their relationships with agricultural crop characteristics. Remote Sensing of Environment. 2000; 71:158–182. https://doi.org/10.1016/S0034-4257(99)00067-X.
16. C.K. Wright, K.M. Beurs, G.M. Henebry. Combined analysis of land cover change and NDVI trends in the Northern Eurasian grain belt. Frontiers of Earth Science. 2012; 6(2):177-187. https://doi.org/10.1007/s11707-012-0327-x.
17. Y.Z. An. W. Gao, Z.Q. Gao, C.S. Liu, R.H Shi. Trend analysis for evaluating the consistency of Terra MODIS and SPOT VGT NDVI time series products in China. Frontiers of Earth Science. 2015;9(1):125-136. https://doi.org/10.1007/s11707-014-0428-9.
18. B. N. Holben, C.O.Justice. An examination of spectral band ratioing to reduce the topographic effect on remotely sense data. International journal of remote sensing. 1981; 2:115-133. https://doi.org/10.1080/01431168108948349.
19. Y.M. Chen, J.X. Gao, Z.Y. Diao, S.H. Lü, X.L. Chang, Z.Y. Feng. Spectral models for estimating grassland vegetation coverage on Hulunbeier grassland, Inner Mongolia, China. China Environmental Science. 2010;30: 1287–1292 (in Chinese with English abstract). http://en.cnki.com.cn/Article_en/CJFDTotal-ZGHJ201009033.htm.

20. P. Sellers. Canopy reflectance, photosynthesis and transpiration. Remote Sensing of Environment. 1985; 21:143–183. https://doi.org/10.1080/01431168508948283.
21. P. Sellers. Canopy reflectance, photosynthesis and transpiration. II. The role of biophysics in the linearity of the interdependence. International journal of remote sensing. 1987;6(8):1335–1372.
22. K. McGwire, Ti. Minor, L. Fenstermaker. Hyperspectral Mixture Modeling for Quantifying Sparse Vegetation Cover in Arid Environments. Remote sensing of environment. 2000; 72:360–374. https://doi.org/10.1016/S0034-4257(99)00112-1.
23. O. Mutanga. Hyperspectral remote sensing of tropical grass quality and quantity. PhD thesis, Wageningen University, Wageningen, The Netherlands. Available online(2004) at: http://library.wur.nl/wda/abstracts/ab3565.html.
24. Chengming Zhang, Jiping Liu, Fan Yu, Shujing Wan, Yingjuan Han, Jing Wang, Gang Wang. Segmentation model based on convolutional neural networks for extracting vegetation from Gaofen-2 images. Appl Remote Sens. 2018;12(4):042804. https://doi.org/10.1117/1.JRS.12.042804.
25. O. Beeri, R. Phillips, J. Hendrickson, A.B. Frank, S. Kronberg. Estimating forage quantity and quality using aerial hyperspectral imagery for northern mixed-grass prairie. Remote Sensing of Environment. 2007;110: 216–225. https://doi.org/10.1016/j.rse.2007.02.027.
26. F. Fava, R. Colombo, S. Bocchi, M. Meroni, M. Sitzia, N. Fois, C. Zucca. Identification of hyperspectral vegetation indices for Mediterranean pasture Characterization. International Journal of Applied Earth Observation and Geoinformation. 2009; 11:233–243. https://doi.org/10.1016/j.jag.2009.02.003.
27. C.J.Tucker. Red and photographic infrared linear combinations for monitoring vegetation. Remote Sensing of Environment. 1979; 8: 127–150. https://doi.org/10.1016/0034-4257(79)90013-0.
28. N.T. Boelman, M. Stieglitz, K.L. Griffin, G.R. Shaver. Interannual variability of NDVI in response to long-term warming and fertilization in wet sedge and tussock tundra. Oecologia. 2005; 143:588−597. https://doi.org/10.1007/s00442-005-0012-9.
29. X. Gao, A. Huete, W. Ni, T. Miura. Optical-biophysical relationships of vegetation spectra without background contamination. Remote Sensing of Environment. 2000; 74: 609−620. https://doi.org/10.1016/S0034-4257(00)00150-4.
30. S.W. Todd, R.M. Hoffer. Responses of spectral indices to variations in vegetation cover and soil background. Photogrammetric Engineering & Remote Sensing. 1998; 64:915−921.
31. K. Kawamura. Quantifying grazing intensities using geographic information system and satellite remote sensing in the Xilingol steppe region, Inner Mongolia, China. Agriculture, Ecosystems and Environment. 2005; 107:83−93. https://doi.org/10.1016/j.agee.2004.09.008.
32. A.R. Huete, C. J.Tucker. Investigation of soil influences in AVHRR red and near-infrared vegetation index imagery. International journal of remote sensing. 1991;12: 1223–1242. https://doi.org/10.1080/01431169108929723.
33. B.R. Zhao, C. Liu, A.J. Liu, Z.X. Wang. Estimate the yield of grassland using MODIS–NDVI – a case study of the grassland in Xilinguole in Inner Mongolia. Pratacultural Science. 2004; 21:12–14 (in Chinese with English abstract). http://en.cnki.com.cn/Article_en/CJFDTotal-CYKX200408003.htm.
34. Z.X. Wang, C. Liu, B.R. Zhao, A.J. Liu. ANPP estimate from Modis-EVI for the grassland region of Xilingol, China. Journal of Lanzhou University (Natural Sciences). 2005; 41:10–16 (in Chinese with English abstract). http://en.cnki.com.cn/article_en/cjfdtotal-ldzk200502003.htm.
35. Z.Q. Du, J. Wang, Y.D. Shen. Estimating model of grassland above-ground biomass based on Remote SensedData in Shandan County. Remote Sensing Technology and Application. 2006;21: 338–343(in

Chinese with English abstract). http://en.cnki.com.cn/Article_en/CJFDTOTAL-YGJS200604012.htm.

36. B.Xu, X.C. Yang. Calculation of grass production and balance of livestock carrying capacity in rangeland region of Northeast China. Geographical Research. 2009; 28:402–408 (in Chinese with English abstract). http://en.cnki.com.cn/Article_en/CJFDTotal-DLYJ200902017.htm.

37. A. Swatantran, R. Dubayah, D. Roberts, M. Hofton, J.B. Blair. Mapping biomass and stress in the Sierra Nevada using lidar and hyperspectral data fusion. Remote Sensing of Environment.2011;115:2917–2930. https://doi.org/10.1016/j.rse.2010.08.027.

38. J.W. Rouse, R.H. Haas, D.W. Deering, J.A. Schell, J.C. Harlan. Monitoring the vernal advancement and retrogradation (green wave effect) of natural vegetation. NASA/GSFC Type III Final Report, Greenbelt, (1974). https://ntrs.nasa.gov/search.jsp?R=19730017588.

39. L.F. Jin, X.R.Xu, M.Zhang. The spectral reflectance model for estimation of green biomass of the typical grassland zone in inner Mongolia. Journal of Inner Mongolia University (Acta Scientiarum Naturalium Universitatis Neimongol).1986;17:735–740 (in Chinese with English abstract). http://en.cnki.com.cn/Article_en/CJFDTotal-NMGX198604019.htm.

40. P.J. Shi, B.Li, Z.H.Li, T.Hu. A research on the production estimation by remote sensing for large area grassland. Acta Agrestia Sinca.1994; 2: 9–12.(in Chinese with English abstract). http://en.cnki.com.cn/Article_en/CJFDTOTAL-CDXU199401001.htm.

41. Y.R.Wang, W.Y Yong. A correlative analysis between near-ground spectral reflectance and yield for Stipa gobica Desert-steppe. Journal of Inner Mongolia University (Acta Scientiarum Naturalium Universitatis Neimongol). 1996;27: 664–669 (in Chinese with English abstract).http://en.cnki.com.cn/Article_en/CJFDTOTAL-NMGX605.017.htm.

42. Mutanga, A.K.SKIDMORE. Narrow band vegetation indices overcome the saturation problem in biomass estimation. International Journal of Remote Sensing. 2004;25: 3999–4014. https://doi.org/10.1080/01431160310001654923.

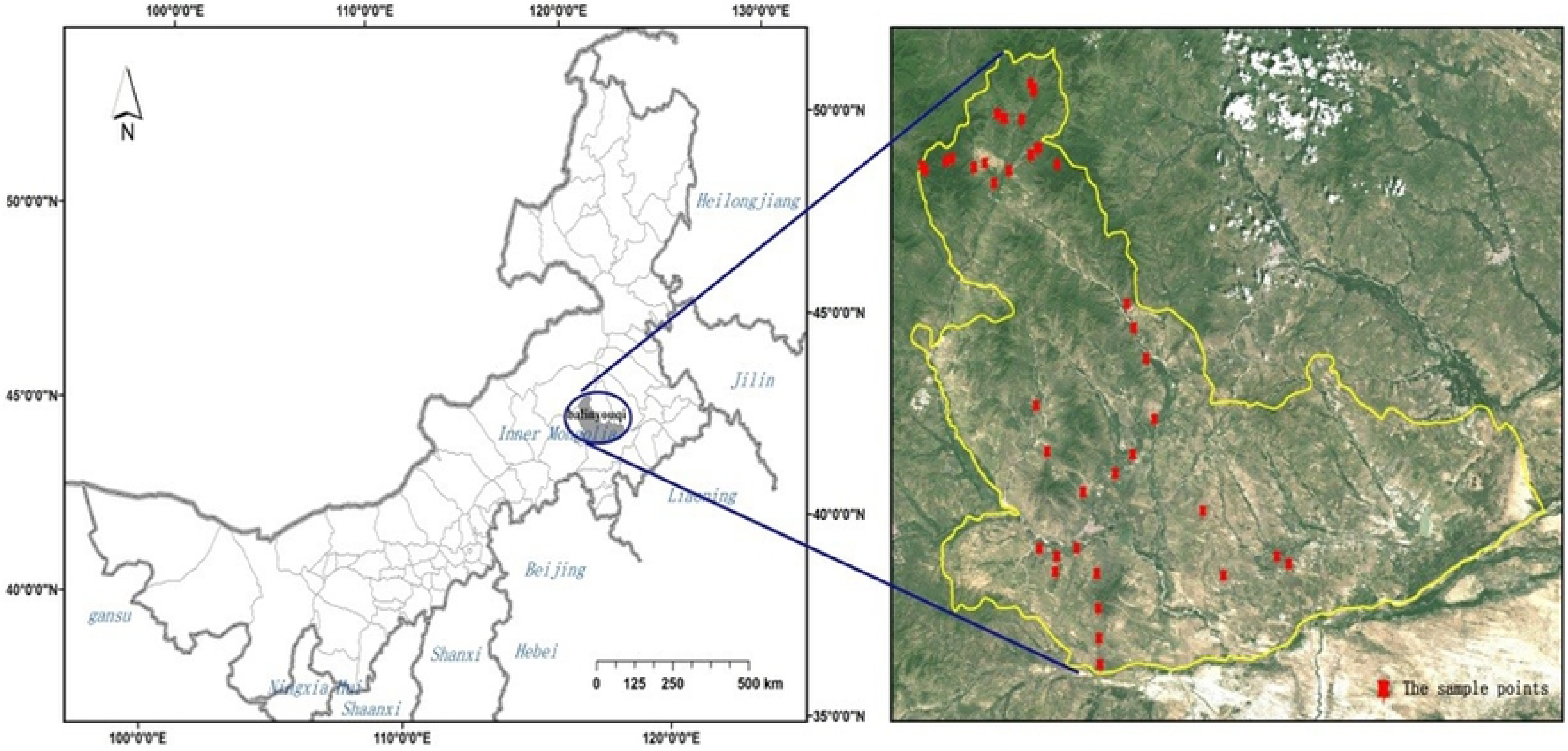

100°0'0"E
110°0'0"E
120°0'0"E
130°0'0"E
N
50°0'0"N
45°0'0"N
40°0'0"N
35°0'0"N
Heilongjiang
Jilin
Inner Mongolia
Liaoning
Beijing
Hebei
Shanxi
Shaanxi
gansu
Ningxia Hui
0 125 250 500 km
The sample points

Figure

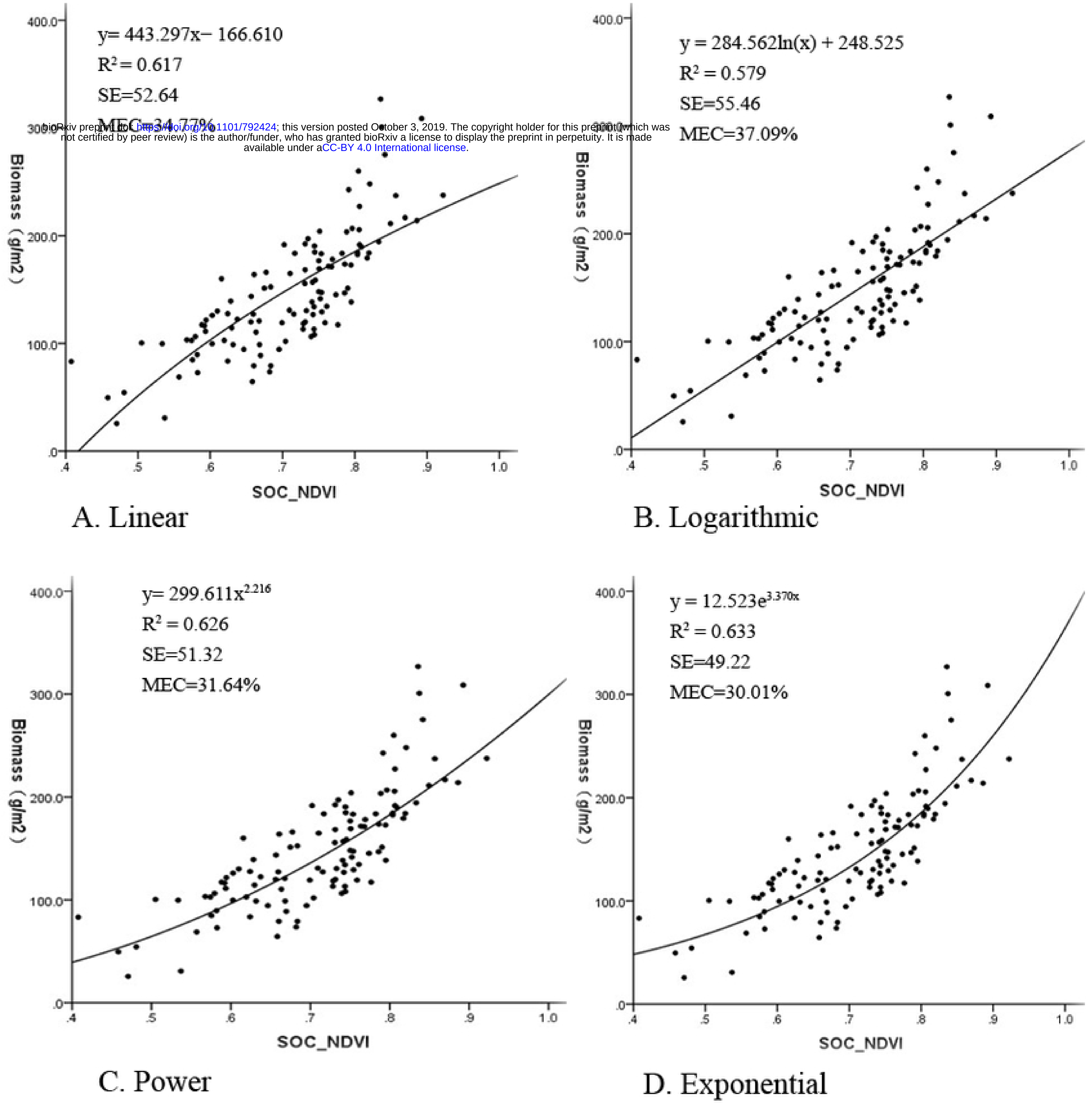
y= 443.297x− 166.610
R² = 0.617
SE=52.64
Biomass（g/m2）
SOC_NDVI
A. Linear
y = 284.562ln(x) + 248.525
R² = 0.579
SE=55.46
MEC=37.09%
B. Logarithmic
y= 299.611x^2.216
R² = 0.626
SE=51.32
MEC=31.64%
C. Power
y = 12.523e^3.370x
R² = 0.633
SE=49.22
MEC=30.01%
D. Exponential

Figure2

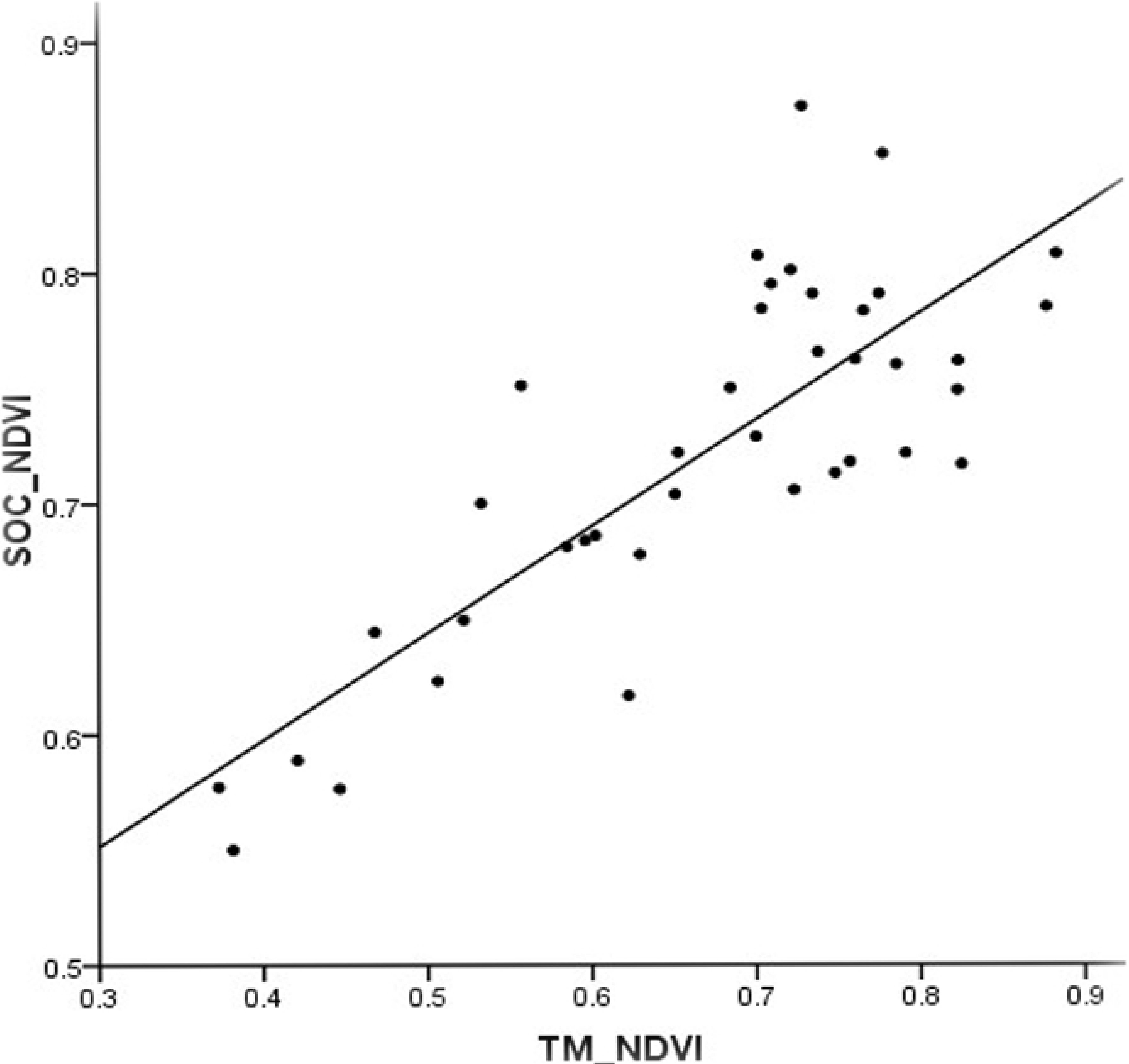

Figure3

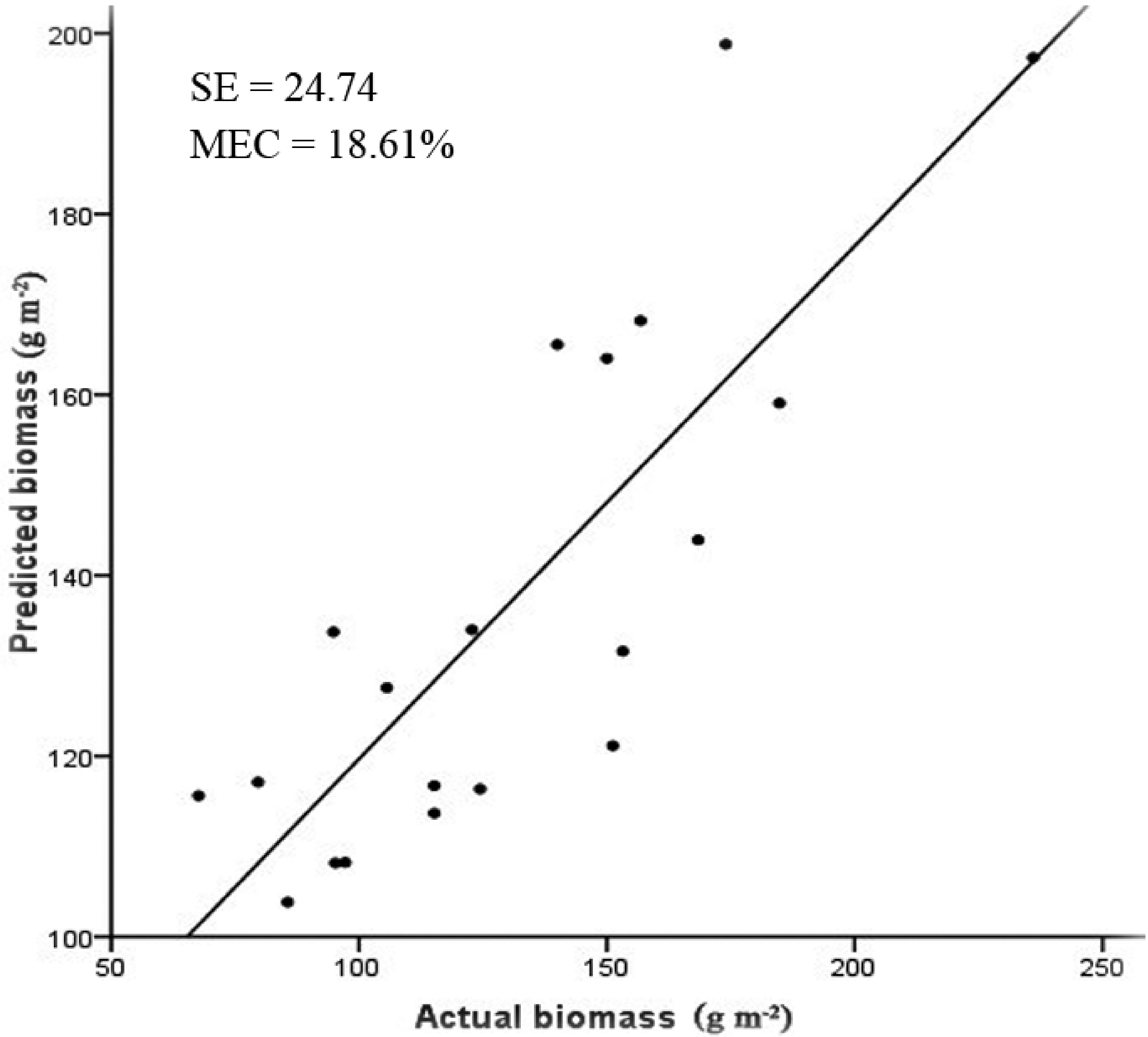
SE = 24.74
MEC = 18.61%
200
180
160
140
120
100
50
100
150
200
250
Predicted biomass (g m⁻²)
Actual biomass (g m⁻²)

Figure4

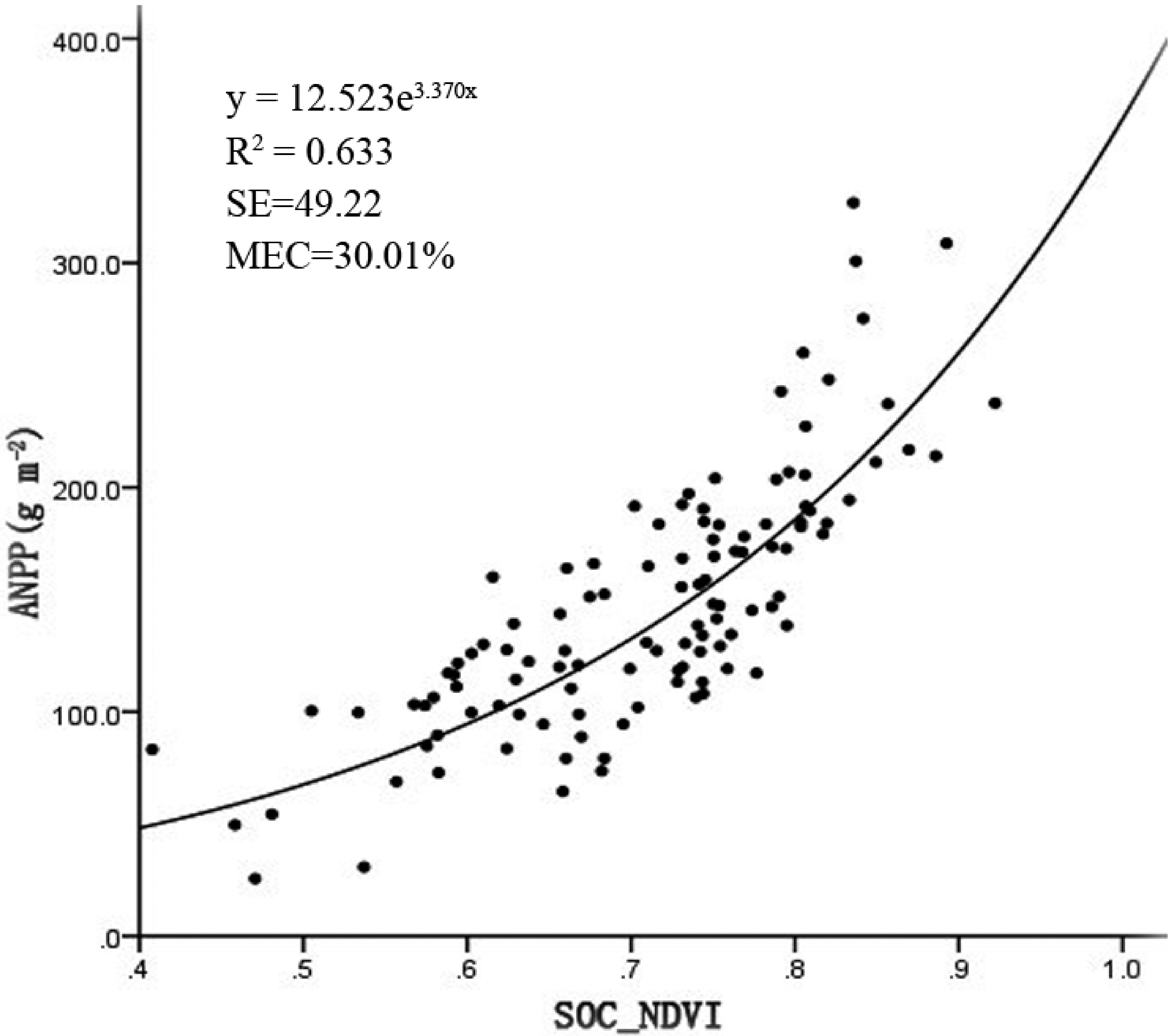

y = 12.523e^3.370x
R^2 = 0.633
SE=49.22
MEC=30.01%
400.0
300.0
200.0
100.0
.0
ANPP (g m^-2)
.4
.5
.6
.7
.8
.9
1.0
SOC_NDVI

Figure5